18

Erosion and Weathering in the Brahmaputra River System

Sunil K. Singh

Planetary Geosciences Division, Physical Research Laboratory, Navrangpura, Ahmedabad 380009, India

18.1 INTRODUCTION

The Brahmaputra is a major river system that flows through very distinct regions: the Tibetan Plateau, the Himalaya Mountains, the Assam Plains, and the delta in Bangladesh. Each of these has its own geology, climate, tectonics, and culture. Compared with other major river basins of Asia, the basin of the Brahmaputra, particularly its upper section, is pristine. Limited accessibility to a number of tributaries of the Brahmaputra, however, has led to a restricted number of studies on the system.

The Brahmaputra plays a significant role in the sediment and element budgets of the globe. It supplies 670 km^3 of water, 1000 million t of particulates, and 100 million t of dissolved material annually to the Bay of Bengal (Milliman and Mead, 1983; Sarin *et al*., 1989; Milliman and Syvitsky, 1992; Hay, 1998). Weathering and erosion rates in the basin are among the highest in the world. The weathered products are delivered to the ocean mostly between June and September when the south-west monsoon operates. The Brahmaputra is a fascinating river system regarding its morphology and operating processes. Floods are common in the river due to intense rainfall, the Assam plain almost invariably gets flooded during every south-west monsoon affecting millions of people. During these floods the Brahmaputra deposits a large volume of sediment along its course but it also removes material, mainly by bank erosion. The large sediment and solute flux transported by the Brahmaputra is a measure of the intense erosion and weathering of its basin, particularly from the mountain reaches. The high physical erosion and chemical erosion in the basin has both regional and global effects. It causes enhanced uplift in mountain ranges and consumption of a disproportionate amount of atmospheric CO_2 (Raymo and Ruddimann, 1992). Weathering in the Brahmaputra and the Ganga Basins contributes significantly to the evolution of seawater chemistry, particularly the Sr and Os isotope systematics and sediment budget (Krishnaswami *et al*., 1992; Pegram *et al*., 1992; Galy *et al*., 1999; Singh *et al*., 2005). Major efforts to investigate weathering and erosion of the Brahmaputra system have been initiated only recently (Singh and France-Lanord, 2002; Singh *et al*., 2003, 2005; Garzanti *et al*., 2004).

This review synthesises the available information on erosion and weathering in the Brahmaputra Basin. Isotopic and elemental data for the particulate and dissolved materials of the Brahmaputra have been taken from Singh and France-Lanord (2002) and Singh *et al*. (2005).

18.2 THE BRAHMAPUTRA RIVER SYSTEM

The source of the Brahmaputra was a matter of great speculation and discussion even a hundred years ago. The Tsangpo in Tibet and the Brahmaputra in India were recognized as the same river only in the late nineteenth century (Montgomerie, 1868). The Brahmaputra is known under different names along its course. Originating in the southern slopes of the snow-covered Kailash Mountain

Large Rivers: Geomorphology and Management, Edited by A. Gupta

(the Jimayangzhong Glacier) in the Trans-Himalaya, it flows eastward on a gentle slope (~0.001) for 1200 km along the Indus-Tsangpo Suture in Tibet known as the Yarlung Tsangpo*,* Tsangpo, Sangpo or Yaluzangbu. The Tsangpo takes a sudden U-turn (Figures 18.1 and 18.2) after Pai at 95 °E around the Namche Barwa Peak of the Eastern Syntaxis curving out a very deep gorge ~5075 m depth. The river then turns south and enters Arunachal Pradesh of India at Singing. This U-turn is also known as 'the Big Bend'. The river is known as the *Siang* or *Dihang* in Arunachal Pradesh, and characterized by a steep gradient (~0.03) and extremely turbulent and rapid flow. The Siang becomes the Brahmaputra in the Assam Plains where it merges with the Dibang and the Lohit (Figures 18.1 and 18.2). In the plains of Assam the Brahmaputra is a wide, deep and braided river that flows in the WWS direction. Turning south near Dhubri the Brahmaputra enters Bangladesh as the Jamuna to meet the Ganga at Arichaghat (see Chapter 19).

The total length of the Brahmaputra from its origin in the Kailash Mountain to Arichaghat is 2900 km. Of this 1600 km is in Tibet, 900 km in India, and the remaining 400 km in Bangladesh (Kumar, 1997). Along its length, the Brahmaputra receives many tributaries. The Lhasa He (Zangbo), Doilung and Nyang Qu (Figure 18.2) are its major tributaries in Tibet. The river also receives several other tributaries draining the northern slope of the Himalaya. The Parlung Zangbo, another tributary with a very high gradient merges with the Tsangpo near the deep gorge after Pai. Figure 18.3 summarizes the long profile and the cumulative discharge of the Brahmaputra.

Flowing through the Assam Plains the Brahmaputra receives many tributaries from the north, east and south. The Subansiri, Ranga Nadi, Jia Bhareli, Puthimari, Manas and Tipkai are some of the north bank tributaries from the Himalaya. The Dibang and Lohit are from the Mishmi Hills to the east, and the Burhi Dihing, Dhansiri and Kopili are from the south (Figure 18.2). The Brahmaputra receives the Tista, a large northern tributary draining the Himalaya, in Bangladesh.

The drainage basin of the Brahmaputra comprises different and contrasting geological and climatic zones. To illustrate, a significant fraction of its drainage is in the dry region of Tibet in the rain shadow of the Himalaya, whereas part of its eastern basin has extremely high rainfall, including Cherrapunji with the highest recorded rainfall (1270 cm year^{-1}) in the world. Average annual temperature varies among the different zones by as much as 40 °C. Lithologies also vary, from easily weathered evaporites to resistant silicates. Along the rivers of the

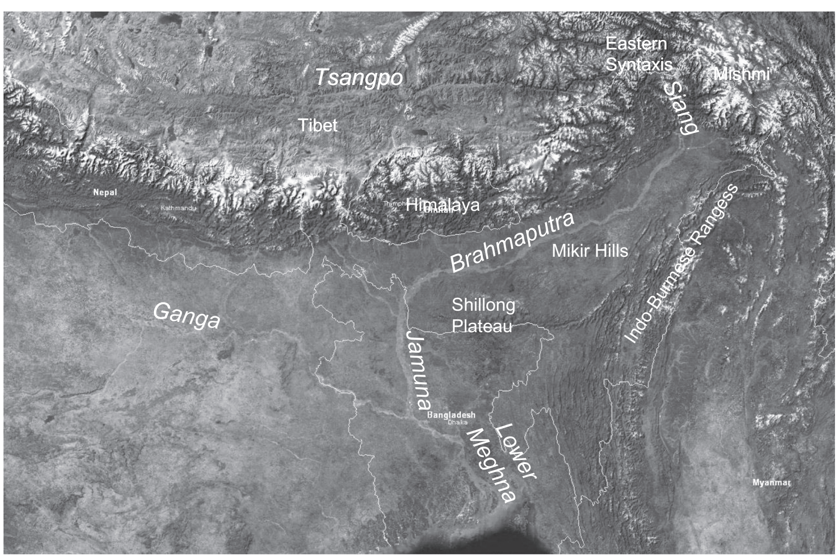

Figure 18.1 Annotated satellite (MODIS) image of the Brahmaputra Basin. The Brahmaputra originates from northern slope of the Himalaya and flows eastward in Tibet. It crosses the Himalaya after taking a U-turn near Namche Barwa. It flows westward in the Assam Plains, and turns south to enter Bangladesh as the Jamuna to join the Ganga. The narrow plain of Assam is bounded by the Himalaya, the Shillong Plateau and Mikir Hills, the Mishmi Hills and the Indo-Burmese (Indo-Myanmar) Ranges (MODIS, Nov. 2004)

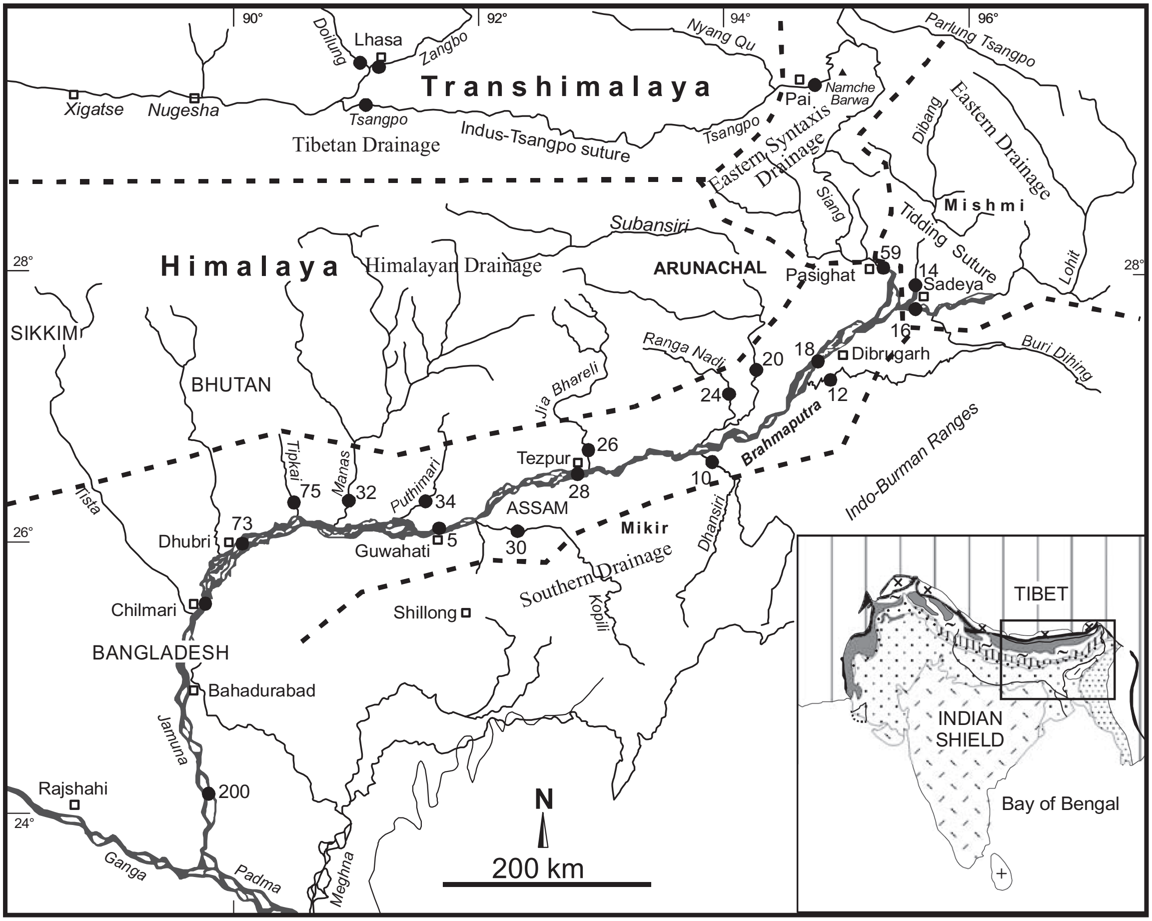

Figure 18.2 The Brahmaputra main stream and its major tributaries in Tibet and in the Assam Plains. Places mentioned in the text and the sampling locations are shown. Reprinted from Geochimica et Cosmochimica Acta, Vol. 69, Singh *et al*., Chemical erosion in the eastern Himalaya: major ion composition of the Brahmaputra and $\delta^{13}C$ of dissolved inorganic carbon, pp. 3573–3588, 2005, with permission from Elsevier

Brahmaputra system, there are sections characterized by some of the highest relief in the world, in contrast there are also sections which have very little relief.

The drainage basin of the Brahmaputra system, from the source to mouth, can be divided into six zones (Figure 18.2):

1. the high plateau of Tibet;
2. the Eastern Syntaxis;
3. the Mishmi Hills or the Eastern Drainage;
4. the Himalaya Mountains;
5. the Indo-Myanmar and Naga-Patkoi Ranges or the Southern Drainage;
6. the plains of Assam and Bangladesh.

18.3 GEOLOGY OF THE BASIN

The geology of the eastern Himalaya is still being studied, but it is possible to summarize the basic lithology of the different sections:

1. *The high plateau of Tibet.* The Tsangpo drains turbidites and ophiolites of the Indus-Tsangpo Suture Zone in its upper reaches in Tibet. The northern tributaries of the Tsangpo drain Trans-Himalayan gabbroic to granodioritic batholiths (Gangdese Belt). Part of the drainage consists of the Lhasa Block which includes Precambrian orthogneisses and metasediments. The Lhasa Block is the southernmost part of Tibet, which was accreted to Asia by a late Jurassic–early Creta-

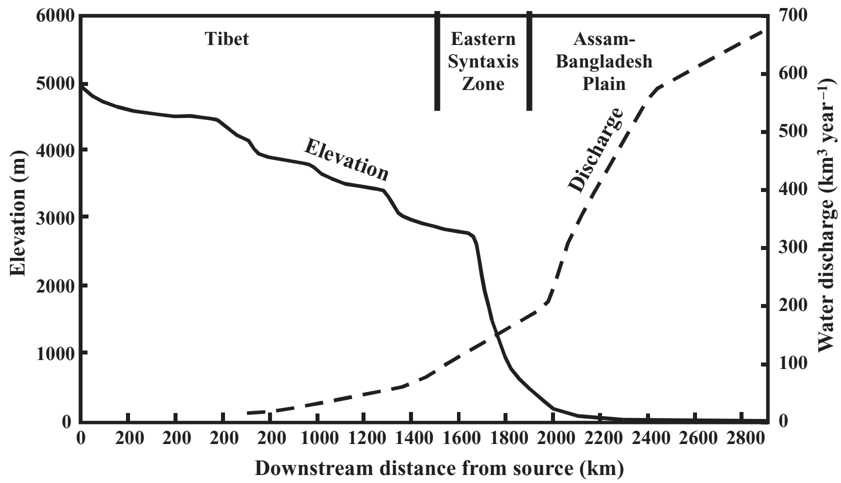

Figure 18.3 Long profile and water discharge of the Brahmaputra main stream. The gradient of the river is very high in the Eastern Syntaxis Zone and the river flows through a very deep gorge (~5000 m). Reprinted from Earth and Planetary Science Letters, Vol. 202, Singh S.K. and France-Lanord, C., Tracing the distribution of erosion in the Brahmaputra watershed from isotopic compositions of stream sediments, pp. 645–662, 2002, with permission from Elsevier

ceous collision after rifting from Gondwana (Booth *et al*., 2004). The tributaries joining the Tsangpo from the south drain the northern slope of the High Himalaya on gneiss and Palaeozoic to Eocene Tethyan sedimentary rocks. Many evaporite deposits and saline lakes are also present in the Tibetan part of the basin (Pascoe, 1963; Hu *et al*., 1982; Pande *et al*., 1994).

2. *The Eastern Syntaxis*. This is the zone where the Tsangpo River makes a U-turn around the Namche Barwa Peak. The rocks of the region are highly metamorphosed. The gneisses of the Indian Plate have been exhumed from below the Trans-Himalayan Plutonic Belt (TPB). These rocks have undergone metamorphism up to upper amphibolite to granulite facies (720–760 °C, 8–10 kb). Quartzites, phyllites and marbles surround the calc-alkaline plutons of the TPB in this zone. This zone is the continuation of the Indus-Tsangpo Suture as indicated by the presence of discrete lenses of metabasites and serpentinites (Burg *et al*., 1998). These are drained by the Siang, Dibang and Parlung Tsangpo.
3. *The Mishmi Hills or the Eastern Drainage*. The two eastern tributaries (the Lohit and Dibang) flow through the Mishmi Hills, the lithology of which includes calc-alkaline diorite-tonalite-granodiorite complexes and tholeiitic metavolcanic rocks of island-arc affinity (Kumar, 1997). It represents the eastern continuation of the TPB, continuing further in Myanmar. The Tidding Suture, the eastern extension of the Indus-Tsangpo Suture with chlorite-schists, amphibolites, and carbonates present in this area, marks the boundary between the TPB and the Himalaya.
4. *The Himalaya Mountains*. In the Brahmaputra Basin, the typical Himalayan formations terminate near the eastern syntaxis against the Tidding Suture. The Siang and other northern tributaries (the Subansiri, Ranga Nadi, Jia Bhareli, Puthimari and Manas) drain the Himalaya to join the Brahmaputra in the plains of Assam. A limited number including the Subansiri originate in the Tethys Himalayan sedimentary zone. The geology of the Himalaya in this section is similar to that of its central and western parts, which is drained by the headwaters of the Ganga. It comprises of the Higher and the Lesser Himalaya and the Siwaliks (Gansser, 1964; Thakur, 1986). The areal proportion of the Lesser Himalaya increases from east to west (Robinson *et al*., 2001; Singh and France-Lanord, 2002). The Higher Himalayan lithologies consist mainly of schists, gneisses, and marbles with amphiboles at some locations. Migmatites and Miocene leucogranites are also common in certain locations. The Manas and Tista drain through metamorphic rocks of the Higher Himalaya in Bhutan and Sikkim. The Lesser Himalaya in the Brahmaputra system is composed mainly of quartzites and schists. Precambrian limestones, dolostones, shales and quartzites along with orthogneiss bodies and dolerite sills are exposed in the Lesser Himalaya. Further south, the Siwalik Hills with thick sections of Neogene molas-

ses are discontinuous in the eastern section of the Himalaya. The Abor Volcanics is present in the Himalayan drainage of the Siang besides the common Himalayan rocks (Jain and Thakur, 1978).

5. *The Indo-Myanmar and Naga-Patkoi Ranges or the Southern Drainage*. These ranges consist mainly of Cretaceous–Eocene pelagic sediments overlain by thick Eocene–Oligocene turbidites associated with Naga ophiolites. These sediments were emplaced onto the eastern India shelf during mid-Tertiary collision with Asia. The southern tributaries (the Dhansiri and Kopili) drain these lithologies along with granite and gneisses of the Indian basement of the Shillong Plateau and the Mikir Hills (Kumar, 1997).
6. *The plains of Assam and Bangladesh*. Part of the plains of Assam and Bangladesh through which the Brahmaputra flows consist of the fluvial sediments brought by the Brahmaputra itself. However, the Indian basement is exposed in some regions in Assam. The floodplain of the Brahmaputra consists of alluvial features such as natural levees, pointbars, ox-bow lakes and channel bars (Goswami, 1998).

18.4 HYDROLOGY

The drainage basin of the Brahmaputra includes contrasting climatic and hydrologic zones. The Tibetan drainage is cold and arid in the rain shadow of the Himalaya. The climate of the rest of the basin is humid subtropical with the temperature varying significantly with altitude. The Assam Plains, the Indo-Myanmar Ranges and the Siwalik section of the Himalaya have hot and humid climate. The Lesser Himalaya and the Mishmi Hills are cooler and wet and the Higher Himalaya, the Tethyan Himalaya and the Eastern Syntaxis are Alpine (Kumar, 1997). Temperatures in Tibet vary from −5.0 to 20 °C (Guan and Chen, 1981). The Brahmaputra Basin outside Tibet has three seasons: summer, wet monsoon, winter. The summer is short, spanning about 2 months (April–May), but the temperature in the plains can rise up to 40 °C. The wet south-west monsoon is active from June to September, except in Tibet. The winter temperature in parts of the plains may drop as low as 0 °C, which is common in the mountains. The peaks of the Higher Himalaya are perennially snow clad.

The annual precipitation is about 300 mm in Tibet, a figure that rises to 5000 mm in the Eastern Syntaxis. Annual rainfall in the southern slopes of the Himalayan drainage of the Brahmaputra is between 1000 and 2000 mm, and over the Mishmi Hills it is about 3000 mm. Monthly precipitation for a period of 10 years (1994–2003) is shown in Figure 18.4 illustrating the seasonality in precipitation. Part of the Himalaya that falls in the rain shadow zone of the Shillong Plateau receives less rainfall. The Naga-Patkoi and Indo-Myanmar Ranges are exposed

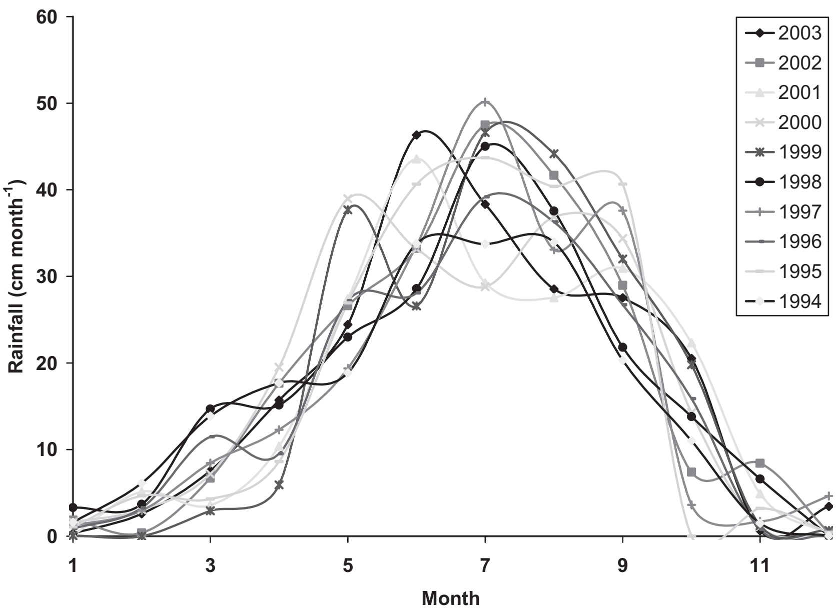

Figure 18.4 Monthly rainfall in north-east India in the Brahmaputra Basin (1994–2003) (from www.tropmet.res.in)

Table 18.1 Discharge and drainage of the Brahmaputra main stream and its tributaries

River	Station	Area (10^5 km^2)	Discharge (km^3 year^{-1})
Brahmaputra main stream			
Tsangpo	Nugesha	1.06	17
Tsangpo	Yangcun	1.53	29
Tsangpo	Nuxia	1.90	59
Tsangpo	Tsela D' Zang	1.91	63
Siang	Pasighat	2.46	200
Brahmaputra	Dibrugarh	2.98	323
Brahmaputra	Pandu	4.05	571
Brahmaputra	Bahadurabad	6.36	670
Tibetan tributaries			
Nyang He	Gyangze	0.06	0.7
Lhasa He	Lhasa	0.26	9.1
Assam Plain tributaries			
Dibang	Sadeya	0.13	63
Lohit	Sadeya	0.24	60
Subansiri	Nr confluence	0.33	54
Ranga Nadi	Nr confluence	0.02	5.8
Jia Bhareli	Nr confluence	0.12	26
Manas	Nr confluence	0.38	32
Puthimari	Nr confluence	0.02	4.4
Burhi Dihing	Nr confluence	0.08	14
Dhansiri	Nr confluence	0.12	20
Kopili	Nr confluence	0.16	28

Source: Rao, 1979; Guan and Chen, 1981; Goswami, 1998; www.grdc.sr.unh.edu.

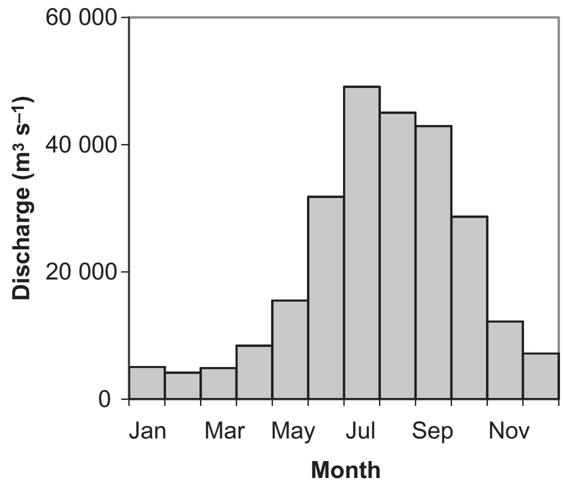

Figure 18.5 Monthly water discharge of the Brahmaputra at Bahadurabad (from www.grdc.sr.unh.edu). Rainfall during the south-west monsoon is the main contributor to annual discharge of the Brahmaputra

to heavy rainfall of 4000 mm year^{-1}. Cherrapunji, which receives the highest rainfall (~13 m year^{-1}) in the world, is located in this region.

Table 18.1 lists the discharge figures of the Brahmaputra main stream and many of its major tributaries and their drainage areas. The discharge of the Brahmaputra at Nugesha, Tibet is 17 km^3 year^{-1} which increases to 60 km^3 year^{-1} before the river enters the syntaxis region. At Bahadurabad in Bangladesh it increases to 670 km^3 year^{-1} (www.grdc.sr.unh.edu). Rainfall is the major source of water for the Brahmaputra, although contributions from meltwater and groundwater are also important during summer. The Tsangpo receives roughly equal contributions from meltwater, groundwater and rainfall (Guan and Chen, 1981). Between June and September, the south-west monsoon contributes 70–80 % of the total discharge of the Brahmaputra. The monthly water discharge pattern of the Brahmaputra at Bahadurabad in Bangladesh reflects the impact of monsoon on the total discharge with significant temporal variation (Figure 18.5).

The total drainage area of the Brahmaputra system is about 630 000 km^2, of which about one-third is in Tibet at an average elevation of 5000 m. The Tibetan drainage contributes about 10 % of the discharge of the Brahmaputra at its mouth. The plains of Assam and Bangladesh together have a drainage area of 200 000 km^2 and the southern slopes of the Himalaya cover an area of 120 000 km^2. About 50 000 km^2 in the Mishmi Hills is drained by the two eastern tributaries, the Lohit and Dibang. The rest of the drainage lies in the Indo-Myanmar and Naga-Patkoi Ranges.

18.5 FLOODS IN THE BRAHMAPUTRA

Floods are a very common annual feature of the Brahmaputra (Figure 18.6). Every year during the south-west monsoon the main stream and the tributaries of the Brahmaputra spill over their banks causing devastating floods in the Assam Plains associated with huge loss and damage to human lives, property, and infrastructure. Large floods with flows in the order of 70 000–100 000 m^3 s^{-1} have a return period of 100 years (Rangachari, 1994; Goswami, 1998). Floods with 25 years recurrence near Guwahati have a discharge of ~60 000 m^3 s^{-1}. In recent times, the highest flood discharge was recorded in 1962 near Guwahati as 73 000 m^3 s^{-1} (Figure 18.6). The average annual flood at Pandu near Guwahati has a magnitude of ~50 000 m^3 s^{-1} with a recurrence period of ~2.6 years (Bhattacharya and Bora, 1997). The bankfull discharge here is 35 000 m^3 s^{-1} which occurs every year on the Brahmaputra (Figure 18.6; Goswami, 1998). The flash floods

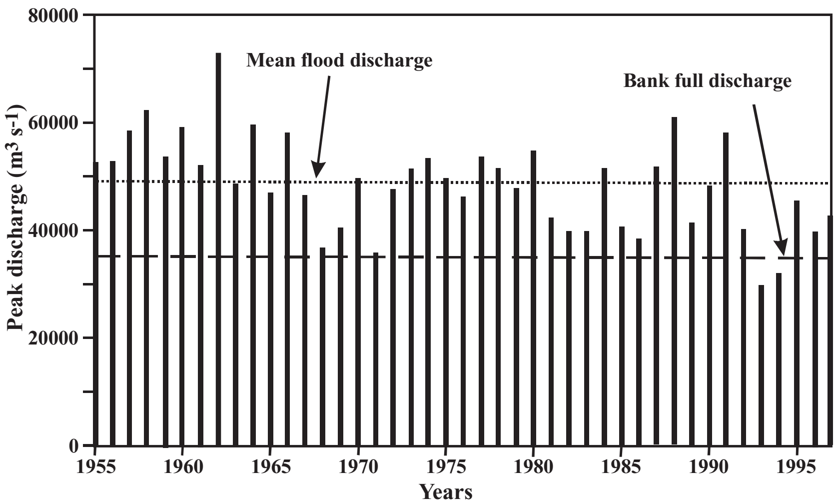

Figure 18.6 Annual peak discharge of the Brahmaputra at Pandu near Guwahati. Levels of bankfull discharge and the mean flood discharge are also shown. Overbank flooding is a yearly phenomenon in the Brahmaputra

of the Himalayan tributaries contribute huge peak discharges leading to flooding of the plains.

During the past 50 years, larger flood events occurred in 1954, 1962, 1966, 1972, 1973, 1977, 1978, 1983, 1984, 1987, 1988, 1991, 1993, 1995, 1996, 1998, 2000 and 2003 (Figures 18.6 and 18.7). More than 10 000 km^2 of land, which is 12.25 % of the geographical area of the state of Assam, is annually affected by floods. The flood of 1998, which inundated 38 000 km^2, about half of Assam, affected the lives and property of about 12.5 million people (Valdiya, 1999). Similarly, 46 500 km^2, including 13 350 km^2 of cropped land was damaged in 1988, affecting tens of millions of people in 10 000 villages (Figure 18.7).

The width of the Brahmaputra Plain in the Assam is about 80 km but the unit flood discharge is extremely high. The high discharge during the south-west monsoon, the restricted width of the valleyflat, and the low gradient in combination result in drainage congestion and floods. The width of the Assam Plains is affected by its northward and eastward underthrusting under the Arunachal Himalaya and the Indo-Myanmar Ranges, respectively (Valdiya, 1999). These tectonic activities cause the Shillong-Mikir Hills of the Peninsular Shield to move closer to the Himalaya, contributing to the narrowing of the plains in Assam. The active deformation of the Assam Plains is evident from the presence of many faults near the Shillong-Mikir Blocks. Most of these faults are seismically active. Valdiya (1999) has observed that the Mikir Block is uplifting rapidly at 31 mm $year^{-1}$, which is indicative of high seismic activity of this area. The uplift of the Shillong Plateau apparently obstructs the Brahmaputra River near Guwahati leading to a narrowing of the valleyflat (Figure 18.8). This along with the deposition of sediment upstream as islands and sandbars in the channel has reduced the carrying capacity of the Brahmaputra.

The Brahmaputra also has a history of flooding due to tectonic disturbances. The massive earthquake of 1897 of magnitude 8.7 partially blocked the flow of the Brahmaputra resulting in huge flooding of the riverine plain. Similarly the earthquake of 1950 (magnitude 8.7) stopped the flow of the Brahmaputra near Dibrugarh causing up to 3 m of siltation on the bed reducing the flow capacity and resulting in more floods in subsequent years (Valdiya, 1999). Anthropogenic activities also contribute to the frequent floods in the Assam Plains. Deforestation in the upper reaches has considerably reduced the resident time of the rainwater in the basin aggravating flood occurrences. The encroachment on the large number of the depressions on the floodplain has reduced the area of natural retention basins. The poorly planned road and railway embankments have also affected the drainage system. The presence of over 4000 km of embankments in the state of Assam, about a third of the total length of embankments in India, illustrates the dependence on structural measures for flood protection (Table 18.2). However, floods on a large river like the Brahmaputra are not very successfully controlled by building embankments. The active tectonics of the Brahmaputra Basin also does not encourage the construction of flood-control structures.

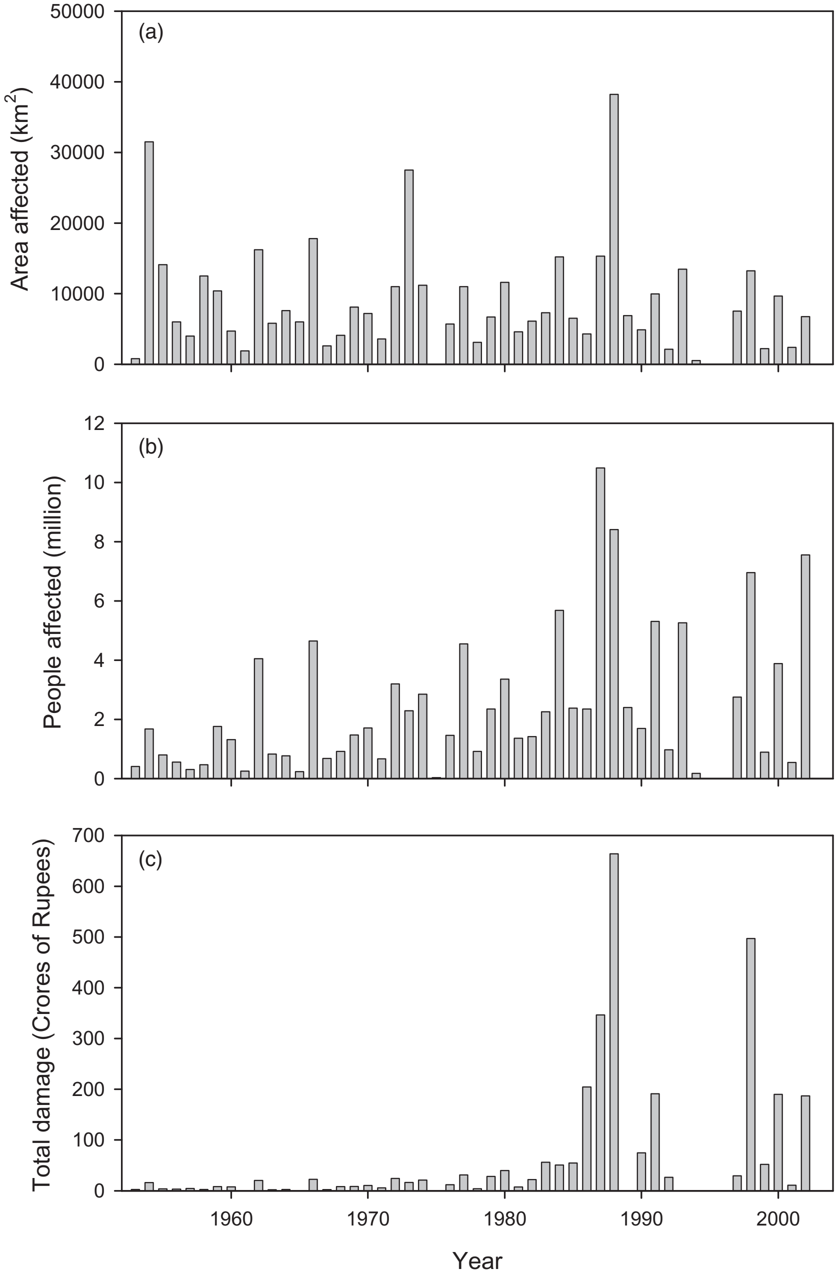

Figure 18.7 Flood effects: (a) area affected; (b) people affected; (c) damage of property (from Goswami, 1998 and Water Resources Department, Assam: www.assamgov.org/Ecosurvey/Flood.htm)

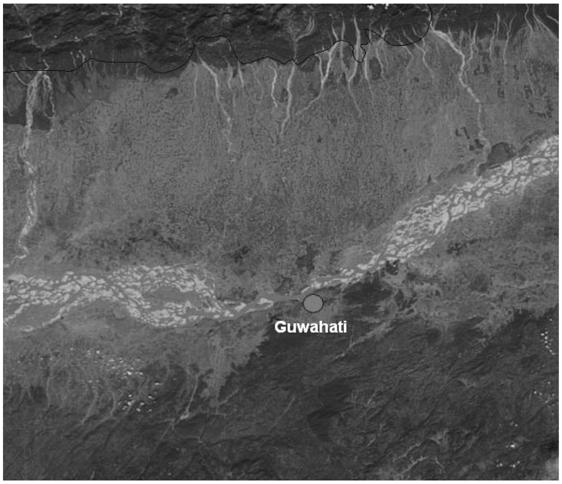

Figure 18.8 MODIS image of narrowed channel of the Brahmaputra mainstream near Guwahati. The continuous uplift and northward movement of the Shillong-Mikir Block has narrowed down the channel of the Brahmaputra near Guwahati, which impounds water flow

Table 18.2 Various flood control measures in Assam

Flood control measures	Dimension
Embankments	4460 km
Drainage channels	850 km
Protection and anti-erosion projects	685
Major sluices	85
Benefited area	16 000 km^2

Source: Water Resources Department, Assam: www.assamgov.org/Ecosurvey/Flood.htm.

Building of upstream storage reservoirs has been considered as an effective flood control measure. The Brahmaputra Board, a statutory body under the Ministry of Water Resources, Government of India, drafted the Brahmaputra Basin Master Plan in 1986 with major emphasis on the construction of large storage reservoirs. The potential sites indicate proposed dams on the Siang, Subansiri and Manas with a total storage capacity of about 70 km^3. The proposals have undergone several modifications over the years. The current plan is to construct three dams each on the Siang and Subansiri. Dams on other rivers (the Pagladiya and the Tipaimukh) are also planned (Water Resources Department, Assam: www.assamgov.org/Ecosurvey/Flood.htm). The slow pace of implementation of these projects seems to indicate that it will take several years before the dams are completed. Besides tectonic activities, the other drawback of these big dams is heavy silting in these rivers. The Rastriya Barh Ayog (National Flood Commission of India) has suggested other structural measure such as the use of natural depressions for moderating the floods and taking anti-erosion measures to protect towns, industrial areas and vital installations.

Such floods are caused mainly by the heavy seasonal runoff, partially blocked by the tectonic configuration of the Assam Plains and reduction of the channel width near the Shillong-Mikir Block. One way to minimize this problem would be to channelize the flood discharge (50 000 $m^3 s^{-1}$; Goswami, 1998) by providing extra passage to these waters through canals, aqueducts or tunnels in the region west of the Mikir Hills (Valdiya, 1999). The canals and river channels would have to be dredged and deepened periodically to take care of uplift and heavy silting. Structural measures, however, are not a complete solution for flood management on the Brahmaputra. There have been suggestions to strengthen the nonstructural methods, such as flood forecasting and warning, flood plain regulation, and disaster release.

18.6 CHARACTERISTICS OF THE BRAHMAPUTRA CHANNEL

The Brahmaputra displays a wide range of morphological variations ranging between steep gorges and wide channels with gentle slopes, probably due to its tectonics-driven gradient changes. The variation in the river slope is shown in Figure 18.3. The gradient of the river in Tibet is variable but, in general, it tends to be low. According to Zhang (2001), the alteration of gentle and steep slopes in Tibet is due to the presence of knickpoints at intervals, which leads to a downstream sequence of sediment accumulation–knickpoint–rapid erosion. Beyond Tibet, the Brahmaputra has cut an ~5000 m deep gorge in the mountains of the Eastern Syntaxis. Its origin has been attributed to rapid erosion, followed by uplift and knickpoint formation (Zeitler *et al*., 2001). The gradient of the Brahmaputra is as steep as 0.03 in the deep gorge but drops to 0.0001 near the Guwahati in the Assam Plains, about 900 km away. In Assam, the average width of the Brahmaputra channel is about 8 km but it does vary. For example, it is only 1 km near Guwahati where hills approach the river. The Brahmaputra acquires a maximum width of 20 km at several locations in the Assam Plains.

The pattern of the channel also varies: meandering, braided, single near-straight. The upper Tsangpo has a freely meandering channel that changes into a braiding pattern downstream. In the middle part of the Tibetan drainage, a single straight channel is common. In the lower part of the river in Tibet, deeply trenched meandering channels flow in gorges. A single meandering channel cuts through the mountain barrier from Pai to Pasighat. Downstream of Pasighat, in the plains of Assam and Bangladesh, the Brahmaputra has a highly braided channel marked by the presence of numerous sandbars and islands (Goswami, 1985). In the Assam Plains the Brahmaputra is characterized by mid-channel bars, sidebars, and tributary mouth bars. Palaeochannels on the interfluves indicate the role of neo-tectonic activities. The plains in Assam and the adjoining hill ranges are seismically very active. Massive earthquakes have occurred in this area, which have changed the course of many rivers of the Brahmaputra system including the main stream (Goswami, 1985). Earthquakes of small magnitudes are a common feature in this area. The channel of the Brahmaputra River has been migrating because of channel widening and avulsion. The Majuli Island in Assam has an area of 600 km^2 between two channels of the Brahmaputra, the largest river island in the world (Kotoky *et al*., 2003). Rapid channel shifts and bank-line recession are characteristic features of the Brahmaputra in the plains.

18.7 EROSION AND WEATHERING

The Brahmaputra supplies large quantities of sediment and solutes to the ocean that amounts to 1000 million t of clastic sediment and 100 million t of dissolved matter annually (Milliman and Meade, 1983; Sarin *et al*., 1989; Milliman and Syvitski, 1992; Hay, 1998; Galy and France-Lanord, 1999; Singh *et al*. 2005). The large quantities of particulate and dissolved matter are derived from a total area of 6 300 000 km^2 (Rao, 1979; Goswami, 1985). The sampling of this river during high flows, especially during floods, is extremely difficult. As sediment transport is expected to peak close to the maximum flow, the paucity of sampling during this period introduces a major uncertainty in ascertaining sediment flux. Sediment budget is commonly based on suspended matter concentration measurements; bedload is hardly ever taken into account. Some of the recent studies (Galy and France-Lanord, 2001) have shown that bedload flux could be a significant part of the total sediment flux in a highly turbulent river such as the Brahmaputra.

Given the high runoff and lithology of the Eastern Himalaya, both physical and chemical erosion rates for the Brahmaputra Basin are higher than those for the Ganga, and much higher than the world average (Sarin *et al*., 1989; Galy and France-Lanord, 2001). Total erosion in the Brahmaputra is about 1.5 to 2 times higher than that of the Ganga (Galy and France-Lanord, 2001). Singh and France-Lanord (2002) and Singh *et al*. (2005) investigated the sources of the clastic sediment and dissolved matter in the Brahmaputra Basin. The erosion rates for the individual zones listed earlier are presented in the following section. The role of various parameters affecting the physical and chemical erosion in the Brahmaputra Basin also has been assessed.

Tracing the sediment in the Brahmaputra Basin is based on the premise that Sr and Nd isotope compositions of the sediments parallel that of their source rocks. The assumption is very likely to be valid for the Himalayan rivers as weathering intensity in these sediments are low (Singh *et al*., 2005). The high water discharge and low residence time of the sediments in the Brahmaputra Basin indicate that weathering in the basin is transport limited (Stallard, 1995) and alteration of the composition of the sediment is low. This is supported by the low proportion of clay in the sediment and the composition of this clay (Singh *et al*., 2005). This suggests that the isotopic composition of the sediments can be considered to be the same as that of the source rocks. To trace the source of sediments, both suspended load and bedload have been collected between Pasighat to Dhubri from the mainstream along with its major tributaries for two seasons: the south-western monsoon and post-monsoon. Samples have been collected from middle of the channel and from sandbars where possible. Care has been taken to collect the representative samples and also to avoid any contamination. The isotopic compositions of these sediments (Table 18.3) have been reported by Singh and France-Lanord (2002) and Singh *et al*. (2003). Figure 18.9 is a mixing plot of sediments based on a two isotope system, $^{87}Sr/^{86}Sr$ and ε_{Nd} (Singh and France-Lanord, 2002). Fields of various end-members present in the basins also have been shown. Sediments of the Brahmaputra main stream fall on the mixing curve between the Higher Himalaya (HH) and the Trans-Himalayan Plutonic Belt (TPB). Apparently about 70 % of the sediment of the Brahmaputra is derived from the HH. Contributions from the TPB and the Lesser Himalaya (LH) are 20 and 10 %, respectively. This confirms the earlier findings of France-Lanord *et al*. (1993) that three-fourths of the sediments of the Bay of Bengal, for which the Brahmaputra is a dominant contributor, carry HH affinity.

Sr, Nd and Os isotope compositions of the sediment of the Brahmaputra main channel are plotted along the river distance in Figure 18.10. It is evident from this plot that the isotopic compositions of these sediments are already determined by the time the river reaches Pasighat, and they hardly vary further downstream. This happens in spite of the Brahmaputra receiving many tributaries below Pasighat, delivering sediment with highly variable isotopic composition. The near-constancy of the isotopic composition of the sediment of the Brahmaputra main channel

Table 18.3 Rb, Sr, Sm, Nd, Re, Os concentrations and Sr, Nd, Os isotope compositions of the sediments of the Brahmaputra River system

Sample	Type	River/Place	Rb (ppm)	Sr (ppm)	$^{87}Sr/^{86}Sr$	Sm (ppm)	Nd (ppm)	ε_{Nd}	Os (ppt)	Re (ppt)	$^{187}Os/^{188}Os$
Brahmaputra main channel											
BR 19	Bank sed.	Dibrugarh	112	243	0.718655	5	28	−12.6	10	70	1.454
BR 19 Clay	Clay	Dibrugarh	224	109	0.72054	6	30	−12.4	–	–	–
BR 29	Bank sed.	Tezpur	116	160	0.728481	7	38	−14.0	13	52	0.969
BR 65SL	Susp. load	Tezpur	196	195	0.719199	7	38	−14.0	43	302	1.07
BR 66	Bank sed	Tezpur	114	157	0.725211	5	26	−13.6	17	57	0.926
BR-2	Susp. load	Guwahati	126	187	0.72105	6	32	−13.0	–	–	–
BR-3	Susp. load	Guwahati	146	175	0.722013	7	37	−13.4	56	275	0.766
BR-4	Susp. load	Guwahati	145	184	0.720567	6	31	−13.2	29	143	0.899
BR-6	Susp. load	Guwahati	147	170	0.720553	7	36	−12.5	57	270	0.834
BR-7	Susp. load	Guwahati	128	211	0.719331	7	37	−13.1	–	–	–
BR-8	Susp. load	Guwahati	129	198	0.719791	6	31	−14.7	–	–	–
BR 9	Bank sed.	Guwahati	83	208	0.717726	8	49	−13.4	15	60	0.835
BR 9 Clay	Clay	Guwahati	235	91	0.717923	8	41	−12.5	–	–	–
BR-52SL	Susp. load	Guwahati	126	232	0.719656	–	22	−13.3	38	359	0.678
BR-53SL	Susp. load	Guwahati	148	167	0.720589	3	–	–	22	419	1.091
BR-54SL	Susp. load	Guwahati	180	194	0.721623	5	–	–	–	–	–
BR-55SL	Susp. load	Guwahati	182	160	0.721859	4	17	−12.8	85	365	0.68
BR-56	Bank sed.	Guwahati	81	244	0.718249	12	66	−13.4	19	75	1.007
BR 73SL	Susp. load	Dhubri	224	148	0.734388	6	31	−14.0	38	210	1.161
BR 74	Bank sed.	Dhubri	100	196	0.721507	6	33	−14.4	17	32	0.64
BGP 14[a]	Bank sed.	Chilamari	126	148	0.734572	7	39	−16.9	12	161	1.596
BGP 82[a]	Bank sed.	Chilamari	74	183	0.721019	9	51	−13.6	18	803	0.815
BGP 18[a]	Susp. load	Chilamari	187	89	0.748838	7	34	−16.3	–	–	–
Eastern tributaries											
BR 15	Bank sed.	Dibang	44	363	0.705296	6	30	−6.9	92	295	0.286
BR 17	Bank sed.	Lohit	33	428	0.70881	9	52	−12.4	40	1040	1.215
Tsangpo											
BR-Ts[b]		Tsangpo	–	–	–	–	38	−10.0	44	230	0.501
T1[c]		Tsangpo	165	277	0.709597	–	–	–	–	–	–
T2[c]		Tsangpo	104	233	0.714306	–	–	–	–	–	–
T3[c]		Tsangpo	109	176	0.715917	–	–	–	–	–	–
T4[c]		Tsangpo	49	670	0.704593	–	–	–	–	–	–

Table 18.3 *Continued*

Sample	Type	River/Place	Rb (ppm)	Sr (ppm)	$^{87}Sr/^{86}Sr$	Sm (ppm)	Nd (ppm)	ε_{Nd}	Os (ppt)	Re (ppt)	$^{187}Os/^{188}Os$
Siang											
BR 59SL	Susp. load	Siang	175	202	0.725241	7	34	–14.6	32	331	1.443
BR 60	Bank sed.	Siang	94	214	0.720604	11	59	–12.0	18	397	2.294
Himalayan tributaries											
BR 21	Bank sed.	Subansiri	89	75	0.735633	7	40	–15.6	16	83	1.048
BR 61SL	Susp. load	Subansiri	127	117	0.730133	6	36	–12.7	36	164	0.9
BR 62	Bank sed.	Subansiri	88	71	0.741897	3	15	–14.1	11	55	1.431
BR 25	Bank sed.	Ranga Nadi	76	89	0.730654	3	20	–12.8	15	142	0.924
BR 58	Bank sed.	Ranga Nadi	106	70	0.738124	3	17	–12.3	11	98	1.07
BR 27	Bank sed.	Jia Bhareli	138	69	0.777051	4	23	–16.3	11	68	1.377
BR 63SL		Jia Bhareli	187	56	0.776816	8	42	–16.6	–	–	–
BR 64	Bank sed.	Jia Bhareli	182	53	0.777346	3	19	–16.4	14	106	1.486
BR 35	Bank sed.	Puthimari	208	61	0.758673	5	30	–17.9	19	180	1.8
BR 69SL		Puthimari	212	69	0.7703	6	36	–17.6	–	–	–
BR 70	Bank sed.	Puthimari	111	39	0.764176	2	10	–17.6	27	141	0.774
BR 33	Bank sed.	Manas	121	70	0.764398	8	45	–16.0	14	63	1.528
BR 71SL	Susp. load	Manas	256	102	0.760045	7	36	–17.2	26	167	1.151
BR 72	Bank sed.	Manas	147	67	0.762298	4	18	–16.4		44	1.21
BR 76	Bank sed.	Tipkai	104	38	0.784524	1	7	–20.2	3	7	1.571
BGP 11[a]		Tista	168	92	0.809621	9	46	–21.2	8	1154	2.859
BGP 76[a]		Tista	226	89	0.824959	8	41	–20.6	–	–	–
Southern tributaries											
BR 31	Bank sed.	Kopili	94	58	0.733421	7	36	–12.7	22	76	0.845
BR 67SL	Susp. load	Kopili	217	85	0.732516	10	55	–15.1	–	–	–
BR 68	Bank sed.	Kopili	37	32	0.736137	17	97	–20.5	10	37	1.003
BR 11	Bank sed.	Dhansiri	77	80	0.718137	6	32	–8.4	49	191	0.471
BR 13	Bank sed.	Buri Dihing	80	129	0.727418	5	29	–18.7	173	35	0.178
BR78	Bank sed.	Basistha Dhara	49	47	0.750154	2	7	–12.6	8	25	6.8
BR 36	Gneiss	Guwahati	115	40	1.076	4	16	–9.5	–	–	–

Source: [a]Galy, 1999; [b]Pierson-Wickman *et al.*, 2000; [c]Harris *et al.*, 1998.

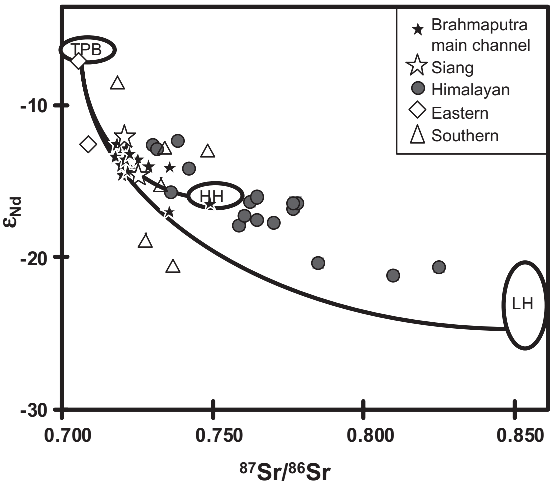

Figure 18.9 Two isotope mixing diagram of the sediments of the Brahmaputra. Also plotted are the fields of the important sources of sediments. The sediment of the Brahmaputra River system is mostly derived from the Higher Himalaya (HH) with a small contribution from the Trans-Himalayan Plutonic Belt (TPB). LH, Lesser Himalaya. Reprinted from Earth and Planetary Science Letters, Vol. 202, Singh S.K. and Fracne-Lanord, C., Tracing the distribution of erosion in the Brahmaputra watershed from isotopic compositions of stream sediments, pp. 645–662, 2002, with permission from Elsevier

from Pasighat to Dhubri at the India–Bangladesh border indicates that sediment derived from upstream of Pasighat determines the sediment characteristics of the Brahmaputra. The proportions of sediment contributed by the various zones in the basin were calculated according to the two end-member mixing model. The results showed that about half of the volume of sediment of the Brahmaputra is derived from upstream of Pasighat (Singh and France-Lanord, 2002). The isotope data and sediment abundance also indicate that the Eastern Syntaxis Zone is the primary contributor of sediment of the river. The contribution from Tibet is low due to factors such as low runoff, gentle slope, and presence of knickpoints on the Tsangpo prior to its entry into the gorge that cuts through the Eastern Syntaxis (Zeitler *et al*., 2001). Material balance calculations based on the isotopic compositions of these sediments show that sediment contribution from Tibet, Eastern Syntaxis, Eastern drainage/Mishmi Hills and the Himalayan basins to the Brahmaputra system are 5, 45, 10 and 40%, respectively (Singh and France-Lanord, 2002). The disproportionately high contribution of sediment from the Eastern Syntaxis Zone to the Brahmaputra system (45%) is striking as it occupies only about 4% of the drainage area.

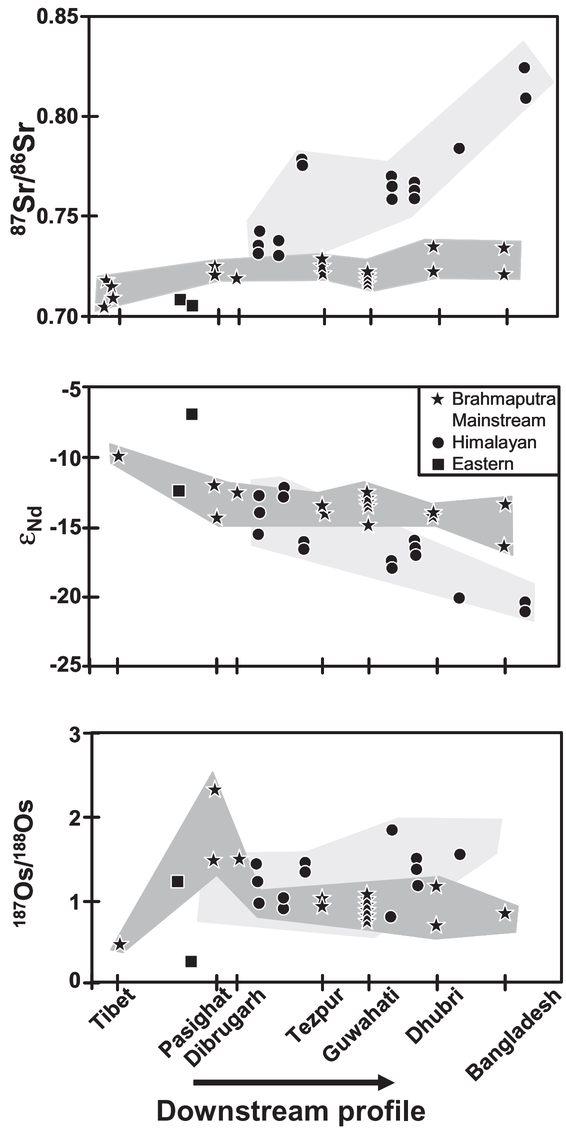

Figure 18.10 Downstream variation of Sr, Nd and Os isotope composition of the Brahmaputra River system. Near constancy of the isotope composition downstream of Pasighat indicates that above-Pasighat sediments are the major contributor to the sedimentary budget of the Brahmaputra system. Reprinted from Earth and Planetary Science Letters, Vol. 202, Singh S.K. and Fracne-Lanord, C., Tracing the distribution of erosion in the Brahmaputra watershed from isotopic compositions of stream sediments, pp. 645–662, 2002, with permission from Elsevier

Various parts of the Brahmaputra Basin have different erosion rates. Sediment yield or the physical erosion rate is the highest in the Eastern Syntaxis Zone and the lowest in Tibet.

18.8 SEDIMENT YIELD OR EROSION RATES IN THE VARIOUS ZONES

The estimates of suspended load flux from the Brahmaputra at Bahadurabad varies from 500 to 1600 million t year^{-1} (Hay, 1998). Studies by Galy and France-Lanord (2001) have shown that due to high energy condition and turbulent flow the fluxes of suspended and bed load are equal in the Ganga and the Brahmaputra Rivers. Considering this, the total annual sediment flux would double to 1000 to 3000 million t. A mean annual sediment flux of 2000 million t has been assumed for the Brahmaputra in order to calculate erosion rates. This flux in conjunction with estimates of sediment proportions from the different zones has been used to derive individual zonal erosion rates (Figure 18.11, Table 18.4). The erosion rates vary from 0.2 mm year^{-1} in Tibet to as high as 14 mm year^{-1} in the Eastern Syntaxis Zone (Singh, 2006). The erosion rate in the Eastern Syntaxis Zone is among the highest in the world (Milliman and Meade, 1983). The Himalayan and the Eastern drainages/Mishmi Hills are eroding at a rate of about 2 mm year^{-1}.

The estimated erosion rates compare well with the available long term erosion or exhumation rates of the Himalayan-Tibetan regions (Table 18.4) For example, the contemporary erosion rate, ~14 mm year^{-1} for the Eastern Syntaxis Zone, is similar to the exhumation rate of 10 mm year^{-1} (Burg *et al*., 1998) in this region for the last 3–4 Ma, and the erosion rate of 9–12 mm year^{-1} reported from the Western Syntaxis using cosmogenic isotopes (Leland *et al*., 1998).

Erosion at a high rate in the Eastern Syntaxis Zone not only supplies a large amount of sediment to the Bay of Bengal but also influences tectonic activity and geomorphology of the region. The intense and focused erosion in the Eastern Syntaxis Zone has contributed to higher uplift of the region because of isostatic rebound which in turn is responsible for the very high peaks of Namche Barwa (7750 m) and Gyala Peri (7150 m). Zeitler *et al*. (2001) is of the opinion that the generation of knickpoints in the river bed of the Tsangpo just before the gorge resulted from the uplift that followed the rapid erosion in this section. The stationary character of the knickpoint despite rapid erosion downstream suggests that the uplift due to the rapid erosion has been sustained for the last 3–4 Ma.

18.9 CHEMICAL WEATHERING AND EROSION

The Brahmaputra River brings, along with particulate matter, large quantities of dissolved solids to the Bay of Bengal (Sarin *et al*., 1989; Singh *et al*., 2005). Studies on the chemistry of river waters have provided a detailed understanding of the sources of dissolved matter in terms

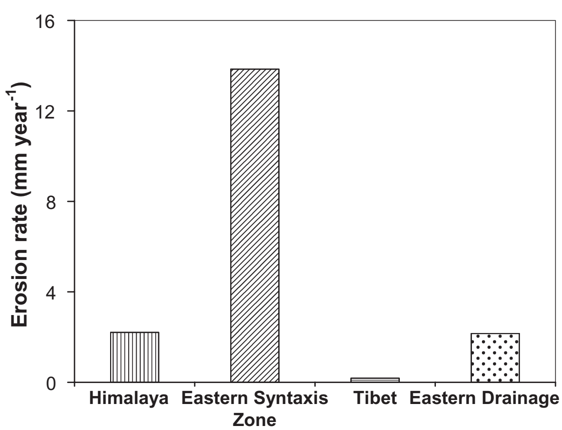

Figure 18.11 Erosion rates of the different parts of the Brahmaputra Basin. Reprinted from Current Science, Vol. 90, Singh, S.K., Copyright 2006, with permission form Current Science

Table 18.4 Erosion and exhumation rates of various regions of the Himalaya

Sub-basins	Erosion rate (mm year^{-1})		Exhumation rate[b] (mm year^{-1})
	Isotope study[a]	Other studies[b]	
Tibet-Tsangpo	0.2	0.01–1.0	–
Higher Himalaya		2.7	1.6–3.0
Lesser Himalaya	2.2	0.8	0.6–1.3
Eastern Syntaxis	14	–	10
Eastern Drainage	2.1	–	–
Nanga Parbat-Indus	–	9–12	4–12

Source: [a] Singh, 2006; [b] data from Burg *et al*., 1998; Leland *et al*., 1998; Lal *et al*., 2003; Vance *et al*., 2003.
Erosion rates are based on cosmogenic isotopes.

of the source area and lithology (Singh *et al*., 2005). These studies have helped also to quantify the weathering rates of silicates, carbonates, and minor lithologies of the basin and the CO_2 consumption due to silicate weathering.

18.9.1 Water Chemistry

The dissolved chemical constituents of river water are derived from the weathering of silicates and carbonates, dissolution of evaporites of the basin, and precipitation. Generally, for the major elements (excluding Cl and Na) the supply from the atmosphere is unlikely to be significant relative to input from chemical weathering of the basin. Even for Na, the significance of rain is likely to be restricted to regions near the sea. In the Brahmaputra system the contribution from precipitation would be negligible, particularly in its headwaters (Galy and France-Lanord, 1999). The total dissolved solids in the waters of the Brahmaputra system ranges between 50 and 182 mg ℓ^{-1} (Table 18.5; Singh *et al*., 2005).

Table 18.5 Major ion composition of waters of the Brahmaputra River system

Sample code	River (location)	Na^+	Na*	K^+	Mg^{2+}	Ca^{2+}	Cl^-	NO_3^-	SO_4^{2-}	HCO_3^-	SiO_2	TDS (mg ℓ^{-1})
		(μmol ℓ^{-1})										
Brahmaputra mainstream												
	Tsangpo (South Lhasa)[a]	396	240	32	209	752	156	–	255	1670	127	185
	Tsangpo (South Lhasa)[a]	446	248	37	191	717	198	–	223	1740	125	187
	Siang (Pai)[b]	387	244	28	103	500	143	–	188	984	125	150
BR-59	Siang or Dihang (Pasighat)	78	61	37	100	424	17	14	119	854	126	95
BR-18	Brahmaputra (Dibrugarh)	106	72	48	144	540	34	–	158	1197	152	128
BR-28	Brahmaputra (Tezpur bg.)	110	86	50	140	458	24	–	110	1154	189	119
BR-65	Brahmaputra (Tezpur bg.)	78	64	49	101	378	14	9	86	845	146	91
	Brahmaputra (Guwahati[1])	159	52	79	119	425	107	–	100	884	123	101
BR-5	Brahmaputra (Guwahati)	86	58	50	115	395	28	–	87	1005	137	102
BR-51	Brahmaputra (Guwahati)	90	69	67	111	475	21	17	114	1051	140	112
BR-73	Brahmaputra (Dhubri)	107	88	50	153	396	19	11	73	1018	200	106
	Brahmaputra (Chilmari)[c]	104	79	52	168	393	25	–	55	1114	155	105
BR 200	Brahmaputra (Jamuna bridge)	77	53	62	120	433	24	–	78	1060	127	105
Tibetan tributaries to Tsangpo												
	Zangbo at Lhasa[a]	380	180	36	39	270	200	–	75	751	134	90
	Doilung at Lhasa[a]	300	38	48	35	224	262	–	60	558	88	73
Eastern tributaries												
BR-14	Dibang	47	33	42	49	353	14	–	82	780	141	82
BR-16	Lohit	59	41	50	78	440	18	–	91	996	139	101
Himalayan tributaries												
BR-20	Subansiri	79	59	24	136	323	20	–	104	849	169	92
BR-61	Subansiri	71	62	26	108	303	9	15	95	667	148	77
BR-24	Ranga Nadi	137	120	33	45	158	17	–	38	550	294	67
BR-57	Ranga Nadi	105	94	28	37	126	11	20	34	373	218	50
BR-26	Jia Bhareli	101	86	32	70	235	15	–	59	682	206	75
BR-63	Jia Bhareli	90	80	32	60	191	10	12	33	537	185	60
BR-75	Tipkai	124	106	27	195	284	18	7	28	994	258	100
BR-32	Manas Biki	97	78	31	148	470	19	–	148	1096	158	117
BR-71	Manas Biki	59	49	27	101	416	10	8	102	844	105	90
BR-34	Puthimari	133	109	43	291	698	24	–	143	1877	218	182
BR-69	Puthimari	99	80	36	219	551	19	19	112	1336	166	135
Southern tributaries												
BR-10	Dhansiri	288	205	63	226	230	83	–	129	881	225	106
BR-12	Buri Dihing	189	147	31	293	228	42	–	85	1084	310	116
BR-30	Kopili	137	104	40	99	158	33	–	65	591	217	70
BR-67	Kopili	118	88	35	78	148	30	3	64	425	208	58

Source: [a]Hu *et al*., 1982; [b]Chen and Guan, 1981; [c]Galy and France-Lanord, 1999.
Na* = ($Na_{riv} - Cl_{riv}$).

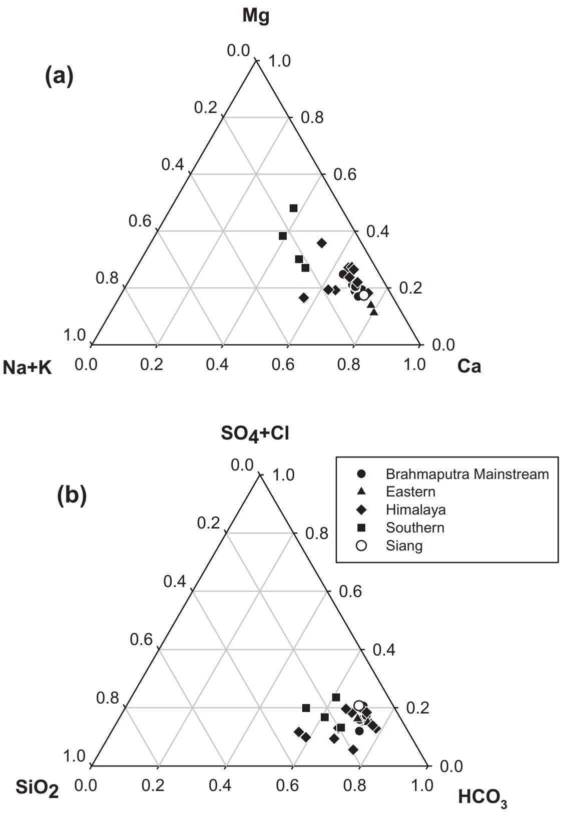

Figure 18.12 Ternary plots of (a) cations and (b) anions of the waters of the Brahmaputra River system showing the dominance of Ca and alkalinity in cations and anions budgets, respectively. Reprinted from Geochimica et Cosmochimica Acta, Vol. 69, Singh *et al.*, Chemical erosion in the eastern Himalaya: major ion composition of the Brahmaputra and $\delta^{13}C$ of dissolved inorganic carbon, pp. 3573–3588, 2005, with permission from Elsevier

Figure 18.12 displays ternary plots of cations and anions in the Brahmaputra waters. Most of the samples fall towards the Ca apex indicating the dominance of Ca in the cation budget of the Brahmaputra. On the anion plot the samples cluster towards HCO_3^- with several of them tending towards the apex with SO_4^{2-}. A preliminary inference from these distributions is that a major source of dissolved cations to the water is carbonate weathering. On a global scale, carbonate weathering contributes about half of the dissolved solids in rivers (Meybeck, 1987).

18.9.2 Silicate Weathering

Weathering of silicate rocks of the drainage basin is another important source of major ions to rivers. Silicate weathering is studied for many reasons, including its role in drawing-down of atmospheric CO_2. Both carbonate and silicate weathering consume CO_2, however, on the million year timescale, CO_2 consumed by carbonate weathering will be released back to the atmosphere during carbonate deposition and hence silicate weathering is the net sink of atmospheric CO_2. Raymo and Ruddimann (1992) hypothesised that the origin and evolution of the Himalaya since the beginning of the Cenozoic has contributed to enhanced silicate weathering rates and hence to increased CO_2 draw-down from the atmosphere. Enhanced uplift coupled with monsoon climate has increased the silicate weathering in the Himalaya which has consumed an increased amount of CO_2 from the atmosphere. As CO_2 is a greenhouse gas, its reduction in atmospheric level has caused global cooling during the Cenozoic. Contemporary silicate weathering and CO_2 consumption rates can be computed from the water chemistry of rivers. This has been done for the Brahmaputra system to assess the significance of this basin compared with other global major river systems. The approach is to derive cation fluxes from silicates from the water chemistry using simple assumptions and use them to calculate CO_2 consumed from the atmosphere. Silicate weathering flux comprises Na, K, Ca, Mg, and SiO_2 derived from the silicate rocks of the basin. What is being measured in the water, however, is derived from multiple sources, and the silicate component has to be separated from the measured values using suitable models. Among the various major ions, SiO_2 and K in rivers are by and large derived from silicates. Na is derived from silicates, evaporites, and precipitation. Na from evaporites and precipitation exists mainly as NaCl, hence sodium from these sources will be accompanied by a similar concentration of chloride. Therefore sodium of silicate origin in rivers can be estimated as:

$$Na_{sil} = Na_r - Cl_r$$

where Na_{sil} is sodium from silicates, and Na_r and Cl_r are sodium and chloride concentrations in rivers, expressed in μE or μM.

Calculating Ca_{sil} and Mg_{sil} from water chemistry is not straightforward, as these cations can be derived from many sources such as silicates, carbonates, and evaporites. Therefore, the contribution of Ca and Mg is calculated assuming that Ca and Mg are released from rocks to rivers in the same proportion as their abundances in silicates or using data on monolithic (silicate basin) tributaries (Krishnaswami *et al.*, 1999). Such calculations show that about 44% of the cations of the Brahmaputra River are of silicate origin (Singh *et al.*, 2005). Based on silicate cations and SiO_2 ($mg\,l^{-1}$) and the specific discharge ($\ell\,km^{-2}$

year^{-1}) of the river, silicate weathering rates were calculated as:

$$\text{Silicate weathering rate} = Q \times (Na_{sil} + K_{sil} + Ca_{sil} + Mg_{sil} + SiO_2)$$

Contemporary silicate weathering rates for the various zones of the Brahmaputra are thus estimated. The rates range from 1 to 38 t km^{-2} year^{-1}, with the Tibetan drainage and the Eastern Syntaxis Zone having the lowest and highest rates respectively. From the silicate cation abundances, present day CO_2 consumption due to silicate weathering in the various zones can also be computed. It varies from 1.9 million mol km^{-2} year^{-1} in the Eastern Syntaxis Zone to 0.07 million mol km^{-2} year^{-1} in Tibet. For the entire Brahmaputra Basin the silicate weathering rate is ~12 t km^{-2} year^{-1} and CO_2 drawdown due to silicate weathering is about 0.6 million mol km^{-2} year^{-1}. Barring the Tibetan drainage, the silicate weathering rates and CO_2 consumption for the entire Brahmaputra and its various parts are significantly higher than the world average (Table 18.6, Figure 18.13). The Eastern Syntaxis Zone has the highest rates of total chemical weathering, silicate weathering, and CO_2 consumption.

18.10 BED LOAD AND WEATHERING INTENSITY

Weathering intensity in the Brahmaputra system can be gauged by the content and composition of the clay in the bed load and their chemical index of alteration (CIA). Low clay content (~2%, except southern tributaries where it is ~20%; Singh *et al.*, 2005) of the bed loads of the Brahmaputra reflects the poor weathering of these sediments which is supported by the dominance of vermiculite in the clay of these sediments. Further the CIA of the sediments of the Brahmaputra range between 58 and 65 (Singh *et al.*, 2005), similar to rocks of the Higher and the Lesser Himalaya. The lower value of CIA of sediments overlaps with those of their source rocks, which indicates that these sediments have undergone low intensity of weathering possibly due to their rapid transport. Sediments of the southern tributaries show higher intensity of weathering.

18.11 CONTROL OF PHYSICAL AND CHEMICAL EROSION IN THE BRAHMAPUTRA BASIN

Variability of an order of magnitude in physical and chemical erosion rates exists among the different zones of the Brahmaputra Basin. A similar variability is also seen when these rates are compared with erosion in major global river basins. A number of factors (climate, basin relief, stream gradient, tectonic activities, lithology, vegetation) have been suggested as controls over erosion rates and their variability (Velbel, 1993; Bluth and Kump, 1994; White and Blum, 1995; Berner and Berner, 1997; Edmond and Huh, 1997; Ludwig and Probst, 1998; Huh and Edmond, 1999; Dalai *et al.*, 2002; Millot *et al.*, 2002;

Table 18.6 Chemical erosion and CO_2 consumption rates in various zones of the Brahmaputra and selected basins of the world

Basin	TDS flux (t km^{-2} year^{-1})	Silicate cation flux (t km^{-2} year^{-1})	CO_2 consumption by silicate weathering (million mol km^{-2} year^{-1})
Brahmaputra			
Tibet	40	1.3	0.07
Eastern Syntaxis	304	38.0	1.9
Eastern	185	18.1	0.95
Himalaya	149	10.7	0.51
Southern	237	22	1.2
Brahmaputra River	120	11.8	0.6
Other Himalayan rivers			
Ganga	72	7.9	0.38
Indus	42	1.8	0.06
Mekong	72	6.2	0.24
Other Tibetan rivers			
Changjiang (Yangtze)	113	1.4	0.06
Huanghe (Yellow)	25	2.1	0.08
Global rivers			
Amazon	35	2.2	0.05
World average	36	2.0	0.09

Source: Sarin *et al.*, 1989; Gaillardet *et al.*, 1999; Singh *et al.*, 2005.

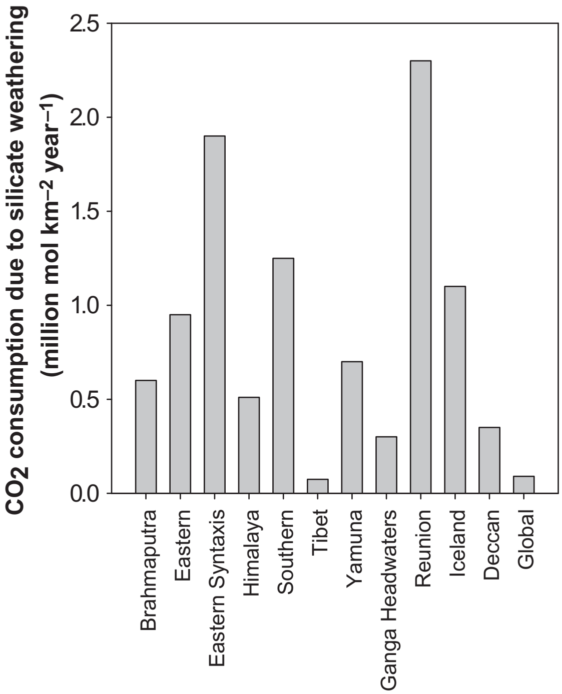

Figure 18.13 CO_2 consumption rates by silicate weathering in the various Himalayan zones as compared with a selection of drainage systems of the world (from Gislason *et al*., 1996; Louvat and Allegre, 1997; Gaillardet *et al*., 1999; Amiotte Suchet *et al*., 2003; Das *et al*., 2005; Singh *et al*., 2005). Reprinted from Geochimica et Cosmochimica Acta, Vol. 69, Singh *et al*., Chemical erosion in the eastern Himalaya: major ion composition of the Brahmaputra and $\delta^{13}C$ of dissolved inorganic carbon, pp. 3573–3588, 2005, with permission from Elsevier

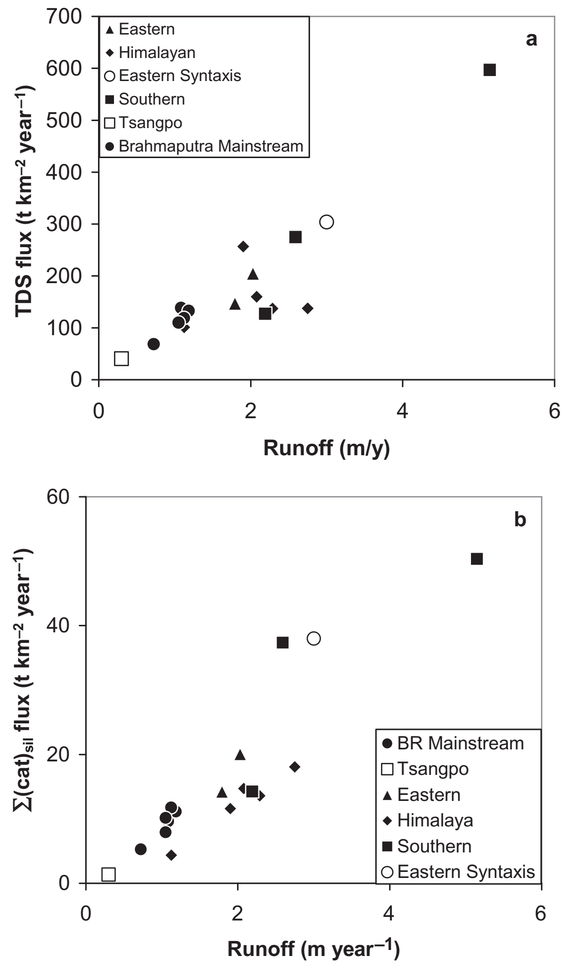

Figure 18.14 Variation of total and silicate erosion rates with runoff in the Brahmaputra River system. Good positive correlation among them shows that the runoff is an important factor controlling the chemical erosion. Reprinted from Geochimica et Cosmochimica Acta, Vol. 69, Singh *et al*., Chemical erosion in the eastern Himalaya: major ion composition of the Brahmaputra and $\delta^{13}C$ of dissolved inorganic carbon, pp. 3573–3588, 2005, with permission from Elsevier

France-Lanord *et al*., 2003). In general, erosion rates in the various parts of the Brahmaputra Basin correlate positively with runoff. However, the disproportionately high erosion rate in the Eastern Syntaxis Zone indicates that than runoff is not the only control over erosion. The river flows in the Eastern Syntaxis Zone over a gradient of 0.03 and an annual discharge of 100 km^3 (Figure 18.3). The stream power of the river is very high in this section. The model on Erosion Index based on stream power of the Brahmaputra (Finlayson *et al*., 2002) supports such an interpretation.

Figure 18.14 shows total chemical weathering and silicate weathering plotted against runoff. The good correlation suggests that chemical erosion in the Brahmaputra system is a function of runoff in the Brahmaputra main channel. The runoff rises by a factor of ten during the south-west monsoon but TDS changes marginally. Chemical and physical erosion of the different zones of the Brahmaputra Basin are plotted against each other in Figure 18.15. The chemical weathering in the different parts of the Brahmaputra is related to the physical erosion of these areas by a power law. In the Brahmaputra Basin, runoff and relief controls physical erosion which in turn controls the chemical erosion by increasing specific surface area for chemical reaction.

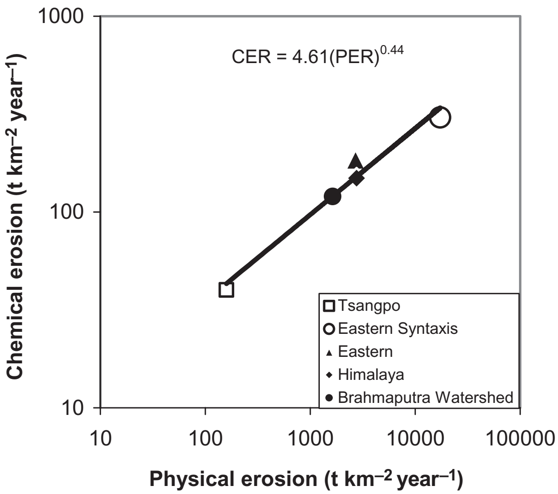

Figure 18.15 Plot of physical erosion rates against chemical erosion rates (CER). In the Brahmaputra system they are related by the power law shown in the figure. Physical erosion felicitates chemical erosion by providing more surfaces. Reprinted from Geochimica et Cosmochimica Acta, Vol. 69, Singh *et al*., Chemical erosion in the eastern Himalaya: major ion composition of the Brahmaputra and $\delta^{13}C$ of dissolved inorganic carbon, pp. 3573–3588, 2005, with permission from Elsevier

18.12 CONCLUSION

The Brahmaputra River system is characterized by high water discharge with high particulate and dissolved matter. Most of its discharge is concentrated in the 4 months of south-west monsoon. Its valley is undergoing uplift near the Shillong-Mikir Block causing narrowing of the valley and congestion to sediment-laden water and hence flooding. Embankments on the Brahmaputra main stream and its tributaries in the Assam Plains seem to be the major flood control measure taken by the government which has turned out to be of limited benefit.

Both physical and chemical erosion rates are high in the Brahmaputra Basin compared with the world average. The erosion rates are highly variable within the basin, with the Eastern Syntaxis Zone and Tibet representing the highest and lowest erosion rates. The Brahmaputra system is contributing significantly to the global CO_2 consumption due to silicate weathering. Erosion in the Brahmaputra seems to be governed by the runoff and the relief of the basin.

REFERENCES

Amiotte Suchet, P., Probst, J.-L. and Ludwig, W. (2003) Worldwide distribution of continental rock lithology: implications for the atmospheric/soil CO_2 uptake by continental weathering and alkalinity river transport to the oceans, *Global Biogeochem. Cycles* 17, 1038.

Berner, E.K. and Berner, R.A. (1997) Silicate weathering and climate. In: *Tectonic Uplift and Climate Change* (W.F. Ruddiman, Ed.), Plenum Press, New York, pp. 354–365.

Bhattacharyya, N.N. and Bora, A.K. (1997) Floods of the Brahmaputra River in India, *Water Int.* 22, 222–229.

Bluth, G.J.S. and Kump, L.R. (1994) Lithologic and climatologic controls of river chemistry, *Geochim. Cosmochim. Acta* 58, 2341–2359.

Booth A.L., Zeitler P.K., Kidd W.S.F., Wooden J., Liu Y., Idleman B., Hren M. and Chamberlain C.P. (2004) U-Pb zircon constraints on the tectonic evolution of southeastern Tibet, Namche Barwa area, *Am. J. Sci.* 304, 889–929.

Burg, J.-P., Nievergelt, P., Oberli, F., Seward, D., Davy, P., Maurin, J.-C., Diao, Z. and Meier, M. (1998) The Namche Barwa syntaxis: evidence for exhumation related to compressional crustal folding, *J. Asian Earth Sci.* 16, 239–252.

Chen, C. and Guan, Z. (1981) Hydrochemistry of rivers in Xizang. In: *Geological and Ecological Studies of Qinghai-Xizang Plateau*, Science Press, Beijing; Gordon and Breach Science Publishers, Inc., New York, pp. 1687–1982.

Dalai, T.K., Krishnaswami, S. and Sarin, M.M. (2002) Major ion chemistry in the headwaters of the Yamuna river system: chemical weathering, its temperature dependence and CO_2 consumption in the Himalaya, *Geochim. Cosmochim. Acta* 66, 3397–3416.

Das, A., Krishnaswami, S., Sarin, M.M. and Pande, K. (2005) Chemical weathering in the Krishna basin and Western Ghats of the Deccan Traps, India: rates of basalt weathering and their controls, *Geochim. Cosmochim. Acta* 69, 2067–2084.

Edmond, J.M. and Huh, Y. (1997) Chemical weathering yields and orogenic terrains in hot and cold climates. In: *Tectonic Uplift and Climate Change* (W.F. Ruddiman, Ed.), Plenum Press, New York, pp. 330–351.

Finlayson, D.P., Montgomery, D.R. and Hallet, B. (2002) Spatial coincidence of rapid inferred erosion with young metamorphic massifs in the Himalayas, *Geology* 30, 219–222.

France-Lanord, C., Derry, L. and Michard, A. (1993) Evolution of the Himalaya since Miocene time: isotopic and sedimentologic evidence from the Bengal Fan. In: *Himalayan Tectonics* (P.J. Treloar and M. Searle, Eds.), Geological Society of London Special Publication 74, Geological Society of London, London, pp. 603–621.

France-Lanord, C., Evans, M., Hurtrez, J.-E. and Riotte, J. (2003) Annual dissolved fluxes from Central Nepal rivers: budget of chemical erosion in the Himalayas, *Comptes Rendus Geosci.* 335, 1131–1140.

Gaillardet, J., Dupre, B. and Allegre, C.J. (1999) Global silicate weathering and CO_2 consumption rates deduced from chemistry of large rivers, *Chem. Geol.* 159, 3–30.

Galy, A. (1999) Etude Geochimique de l'erosion Actuelle de la Chaine Himalayenne, Thesis, Institut National Polytechnique de Lorraine, Nancy.

Galy, A. and France-Lanord, C. (1999) Weathering processes in the Ganges-Brahmaputra basin and the riverine alkalinity budget, *Chem. Geol.* 159, 31–60.

Galy, A. and France-Lanord, C. (2001) Higher erosion rates in the Himalaya: geochemical constraints on riverine fluxes, *Geology* 29, 23–26.

Galy, A., France-Lanord, C. and Derry, L.A. (1999) The Strontium isotopic budget of Himalayan rivers in Nepal and Bangladesh, *Geochim. Cosmochim. Acta* 63, 1905–1925.

Gansser, A. (1964) *Geology of the Himalaya*, Interscience Publishers, London.

Garzanti, E., Vezzoli, G., Andò, S., France-Lanord, C., Singh, S.K. and Foster, G. (2004) Sand petrology and focused erosion in collision orogens: the Brahmaputra, *Earth Planet. Sci. Lett.* 220, 157–174.

Gislason, S.R., Amorsson, S. and Armannsson, H. (1996) Chemical weathering of basalt as deduced from the composition of precipitation, rivers, and rocks in SW Iceland, *Am. J. Sci.* 296, 837–907.

Goswami, D.C. (1985) Brahmaputra River, Assam, India: physiography, basin denudation, and channel aggradation, *Water Resources Res.* 21, 959–978.

Goswami, D.C. (1998) Fluvial regime and flood hydrology of the Brahmaputra River, Assam. In: *Flood Studies in India* (V.S. Kale, Ed.), Geological Society of India, Bangalore, pp. 51–75.

Guan Z. and Chen, C. (1981) Hydrographical features of the Yarlung Zangbo River. In: *Geological and Ecological Studies of Qinghai-Xizang Plateau*, Science Press, Beijing; Gordon and Breach Science Publishers, Inc., New York, pp. 1693–1703.

Harris, N., Bickle, M., Chapman, H., Fairchild, I. and Bunbury, J. (1998) The significance of the Himalayan rivers for silicate weathering rates: evidence from the Bhote Kosi tributary, *Chem. Geol.* 144, 205–220.

Hay, W.W. (1998) Detrital sediment fluxes from continents to oceans, *Chem. Geol.* 145, 287–323.

Hu, M., Stallard, R.F. and Edmond, J. (1982) Major ion chemistry of some large Chinese Rivers, *Nature* 298, 550–553.

Huh, Y. and Edmond, J. (1999) The fluvial geochemistry of rivers of Eastern Siberia: III. Tributaries of the Lena and Anbar draining the basement terrain of the Siberian Craton and the Trans-Baikal Highlands, *Geochim. Cosmochim. Acta* 63, 967–987.

Huh, Y, Tsoi, M.-Y., Zaitsev, A. and Edmond, J. (1998) The fluvial geochemistry of the rivers of Eastern Siberia: I. Tributaries of the Lena River draining the sedimentary platform of the Siberian Craton, *Geochim. Cosmochim. Acta* 62, 1657–1676.

Jain, A.K. and Thakur, V.C. (1978) Abor volcanics of the Arunachal Himalaya, *J. Geol. Soc. India* 19, 335–349.

Kotoky, P., Bezbaruah, D., Baruah, J. and Sarma, J.N. (2003) Erosion activity on Majuli – the largest river island of the world, *Current Sci.* 84, 929–932.

Krishnaswami, S., Trivedi, J.R., Sarin, M.M., Ramesh, R. and Sharma, K.K. (1992) Strontium isotopes and rubidium in the Ganga-Brahmaputra river system: Weathering in the Himalaya, fluxes to the Bay of Bengal and contribitions to the evolution of oceanic $^{87}Sr/^{86}Sr$, *Earth Planet. Sci. Lett.* 109, 243–253.

Krishnaswami, S., Singh, S.K. and Dalai, T. (1999) Silicate weathering in the Himalaya: role in contributing to major ions and radiogenic Sr to the Bay of Bengal. In: *Ocean Science, Trends and Future Directions* (B.L.K. Somalyajulu, Ed.), Indian National Science Academy and Akademia International, New Delhi, pp. 23–51.

Kumar, G. (1997) *Geology of the Arunachal Pradesh*, Geological Society of India, Bangalore.

Lal, D., Harris, N.B.W., Sharma, K.K., Gud, Z., Ding, L., Liu, T., Dong, W., Caffee, M.W. and Jull, A.J.T. (2003) Erosion history of the Tibetan Plateau since the last interglacial: constraints from the first studies of cosmogenic ^{10}Be from Tibetan bedrock. *Earth Planet. Sci. Lett.* 217, 33–42.

Leland, J., Reid, M.R., Burbank, D.W., Finkel, R. And Caffee, M. (1998) Incision and differential bedrock uplift along the Indus River near Nanga Parbat, Pakistan Himalaya, from Be and Al exposure age dating of bed rock straths, *Earth Planet. Sci. Lett.* 157, 93–107.

Louvat, P. and Allegre, C.J. (1997) Present denudation rates on the island of Reunion determined by river chemistry: basalt weathering and mass budget between chemical and mechanical erosions, *Geochim. Cosmochim. Acta* 61, 3645–3699.

Ludwig, W. and Probst, J.-L. (1998) River sediment discharge to the oceans: present-day controls and global budgets, *Am. J. Sci.* 298, 265–295.

Meybeck, M. (1987) Global chemical weathering of surficial rocks estimated from river dissolved loads, *Am. J. Sci.* 287, 401–428.

Milliman, J.D. and Meade, R.H. (1983) World Delivery of River Sediment to the Oceans, *J. Geol.* 91, 1–21.

Milliman, J.D. and Syvitski, P.M. (1992) Geomorphic/tectonic control of sediment discharge to the ocean: the importance of small mountainous rivers, *J. Geol.* 100, 525–544.

Millot, R., Gaillardet, J., Dupré, B. and Allègre, C.J. (2002) The global control of silicate weathering rates and the coupling with physical erosion: new insights from rivers of the Canadian Shield, *Earth Planet. Sci. Lett.* 196, 83–98.

Montgomerie, T.G. (1868) Report of a route survey made by pundit, from Nepal to Lhasa, and thence through the upper valley of the Brahmaputra to its source, *J. R. Geograph. Soc. London* 38, 129–219.

Pande, K., Sarin, M.M., Trivedi, J.R., Krishnaswami, S. and Sharma, K.K. (1994) The Indus river system (India-Pakistan): major-ion chemistry, uralium and strontium isotopes, *Chem. Geol.* 116, 245–259.

Pascoe, E.H. (1963) *A Manual of the Geology of India and Burma*, Vol. 3, Government of India Press, Calcutta, pp. 2073–2079.

Pegram, W.J., Krishnaswami, S., Ravizza, G.E. and Turekian, K.K. (1992) The record of sea water $^{187}Os/^{186}Os$ variation through the Cenozoic, *Earth Planet. Sci. Lett.* 113, 569–576.

Pierson-Wickman, A.-C., Reisberg, L. and France-Lanord, C. (2000) The Os isotopic composition of Himalayan river bedloads and bedrocks: importance of black shales, *Earth Planet. Sci. Lett.* 176, 203–218.

Rangachari, R. (1994) Flood management. In: *Harnessing the Eastern Himalayan Rivers Regional Cooperation in South Asia* (Editors B.G. Vergese and R. Ramaswamy Iyer), Konark Publishers Pvt Ltd, Delhi, pp. 86–98.

Rao, K.L. (1979) *India's Water Wealth*, Orient Longman Limited, New Delhi.

Raymo, M.E. and Ruddiman, W.F. (1992) Tectonic forcing of late Cenozoic climate, *Nature* 359, 117–122.

Robinson, D.M., DeCelles, P.G., Patchett, P.J. and Garzione, C.N. (2001) The kinematic evolution of the Nepalese Himalaya interpreted from Nd isotopes, *Earth Planet. Sci. Lett.* 192, 507–521.

Sarin, M.M., Krishnaswami, S., Dilli, K., Somayajulu, B.L.K.and Moore, W.S. (1989) Major ion chemistry of the Ganga-Brahmaputra river system: weathering processes and fluxes to the Bay of Bengal, *Geochim. Cosmochim. Acta* 53, 997–1009.

Singh, S.K., (2006) Spatial variability in erosion in the Brahmaputra basin: causes and impacts, *Curr. Sci.* 90, 1272–1276.

Singh, S.K. and France-Lanord, C. (2002) Tracing the distribution of erosion in the Brahmaputra watershed from isotopic compositions of stream sediments, *Earth Planet. Sci. Lett.* 202, 645–662.

Singh, S.K., Reisberg, L. and France-Lanord, C. (2003) Re-Os isotope systematics of sediments of the Brahmaputra River system, *Geochim. Cosmochim. Acta* 67, 4101–4111.

Singh, S.K., Sarin, M.M. and France-Lanord, C. (2005) Chemical erosion in the eastern Himalaya: major ion composition of the Brahmaputra and $\delta^{13}C$ of dissolved inorganic carbon, *Geochim. Cosmochim. Acta* 69, 3573–3588.

Stallard, R.F. (1995) Tectonic, environmental, and human aspects of weathering and erosion: a global review using a steady-state perspective. *Ann. Rev. Earth Planet. Sci.* 23, 11–39.

Thakur, V.C. (1986) Tectonic zonation and regional framework of eastern Himalaya, *Science Terre* 47, 347–360.

Valdiya, K.S. (1999) Why does river Brahmaputra remain untamed?, *Curr. Sci.* 76, 1301–1304.

Vance, D., Bickle M., Ivy-Ochs, S. and Kubik, P.W. (2003) Erosion and exhumation in the Himalaya from cosmogenic isotope inventories of river sediments, *Earth Planet. Sci. Lett.* 206, 273–288.

Velbel, M.A. (1993) Temperature dependence of silicate weathering in nature: how strong of a negative feedback on long term accumulation of atmospheric CO_2 and global greenhouse warming?, *Geology* 21, 1059–1062.

White, A.F. and Blum, A.E. (1995) Effects of climate on chemical weathering in watersheds. *Geochimica et Cosmochimica Acta* 59, 1729–1747.

www.grdc.sr.unh.edu

www.tropmet.res.in

Zeitler, P.K., Meltzer, A.S., Koons, P.O., Craw, D., Hallet, B., Chamberlain, C.P., Kidd, W.S.F., Park, S.K., Seeber, L., Bishop, M. and Shroder, J. (2001) Erosion, Himalayan geodynamics, and the geomorphology of metamorphism, *GSA Today*, 4–9.

Zhang, D.D. (2001) Tectonically controlled fluvial landforms on the Yaluzangbu River and their implications for the evolution of the river, *Mountain Res. Dev.* 21, 61–68.